Journal of Sound and Vibration (1976) **48**(4), 485–510

THE ACOUSTIC TELESCOPE

J. BILLINGSLEY AND R. KINNS†

Department of Engineering, University of Cambridge, Cambridge CB2 1PZ, England

(*Received* 28 *October* 1975, *and in revised form* 3 *June* 1976)

A system has been developed for real-time sound source location on full-size jet engines. It consists of an array of microphones connected to a small digital computer, via a sequence of preamplifiers, analog filters and analog to digital converters and multiplexer. Microphone signals can be processed on-line to give displays of time varying source distributions or statistical averages with respect to position and frequency, by using a colour television as well as a display screen and printer/plotter. The whole system can be transported in a small estate car and can be used on both model scale and full size engine test rigs.

A theoretical analysis of system performance is in terms of a line source of generally correlated omni-directional sound radiators, which shares the measurable far-field properties of a jet engine noise source. The general properties of the system are described, including its use to correlate spatially separated sound sources, application in the presence of ground reflections and use in a moving airstream. The statistical properties of apparent source distributions are also discussed.

A series of experiments on a Rolls-Royce/SNECMA Olympus engine is described, in order to illustrate application of the system.

1. INTRODUCTION

Public opinion demands quieter turbojet engines. As a result there has been a huge investment in research programmes to enable a better understanding of noise generation processes. It was felt at an early stage that if more were known of the apparent origin of the noise field from a jet engine source, there should be a sounder base for reducing that noise field.

However, Ffowcs Williams [1] has emphasized that there is no unique specification to the origin of a given wave field and that it is only possible to define an equivalent source distribution which shares the measureable far-field properties of the real noise source. Even then, the complex phenomena associated with the sound generation and propagation require a mathematical model which can simulate a source region with high directionality and arbitrary correlation of sources with respect to their separation. The non-uniqueness of the origin of a specified wave field is fundamental, but proper recognition of the properties of that field is essential to its interpretation.

Various techniques have been proposed for identification of this apparent source distribution. Acoustic mirrors have been used at model scale in anechoic chambers. Usually an ellipsoidal mirror is used with a microphone at one focus and the investigated point at the other. To move the second focus, the entire mirror must be displaced (see, e.g., reference [2]), or rotated. The apparent source distribution is usually deconvolved with respect to the "image" of a monopole source on the assumption that this is reasonable for a directional source region. However, such apparatus is practically impossible to apply at engine scale, owing to its bulk and the more demanding environment in which it must be used. Multiple microphone techniques appear much more attractive, owing to the ease with which micro-

† Present address: Y-ARD Limited, Charing Cross Tower, Glasgow G2 4PP, Scotland.

phone configurations can be altered and to the availability of high speed data processing techniques.

The development of a procedure for the interpretation of signals from a pair of closely spaced microphones has been described by Kinns [3], while Fisher and Harper Bourne [4] describe a technique for transformation of correlation data from a polar array of microphones. A fixed microphone array dedicated to a single focus had also been used by the General Electric Company [5]. However, radio astronomy techniques pioneered in Cambridge demonstrated that a microphone array can be focused, merely by the way in which the signals are processed. The focus can be varied at will, with no mechanical adjustment. Indeed, the same data can furnish information for an array of foci.

A system was developed for sound source location which uses a line array of fourteen microphones. At a prototype stage [6] processing was performed off-line and the system was applied to a Rolls-Royce Viper engine [7]. Field experience and theoretical developments have led to the present system which can be used for on-line analysis by using a mini-computer. It can be used to determine the statistical properties of a source region, including the correlation of sound sources in both time and frequency domains. It can also resolve the separate events which lead to the overall properties.

The design and construction of the data processing system is described first. The basic properties of the analysis for various simple test situations are then considered, while a formal frequency domain analysis is presented for the case of a line source of arbitrarily correlated sound radiators. This mathematical model for the source region shares the measureable far-field properties of a real jet engine noise source and provides a basis for interpretation. The uses of the system in the presence of ground reflections, in a wind tunnel for the investigation of flight effects, and for estimation of the correlation between separated sound sources, are described.

Finally, results from tests on a Rolls-Royce/SNECMA Olympus engine are presented in order to illustrate the use of the system for frequency domain analysis.

2. APPARATUS

Figure 1 shows a block diagram of the signal processing system. Signals from the microphones and preamplifiers pass to the main amplifiers before filtering, quantization, computation and display.

The condenser microphones are 6·35 mm Brüel and Kjaer type 4135, energized at 150 volts. Their weak output, 0·15 millivolts per μbar, from an impedance of 6 pF, necessitates a very high input impedance preamplifier to obtain a flat response down to 30 Hz. The upper frequency limit of the system is 80 kHz. The preamplifier has a gain which can be remotely switched, to maintain a reasonable signal level on the 100 metre cable between microphones and central console. Each preamplifier is housed within a 25·4 mm diameter tube which forms part of the microphone mounting. The microphone capsule is located at the end of a length of 6·35 mm tube, blended to the 25·4 mm tube with a shallow conical section. Individual microphone cables gather to a nearby junction box and these are connected by two multiple cables to the central unit. This unit has gain controls for each channel, allowing switching in 10 dB steps to allow recordings of sound pressure levels between 60 dB and 140 dB relative to 2×10^{-4} μbar. Connections are provided for record and replay to an Ampex FR-1300A 14-channel tape recorder, so that recordings may be made for off-line analysis. However, the recorder is not essential to the system.

Signals then pass to an anti-aliasing filter circuit, containing fourteen channels of low-pass filters. These are six-pole Butterworth, with a range of six frequencies which are switched automatically so that they have 3 dB attenuation at half the data sampling rate. Next, the

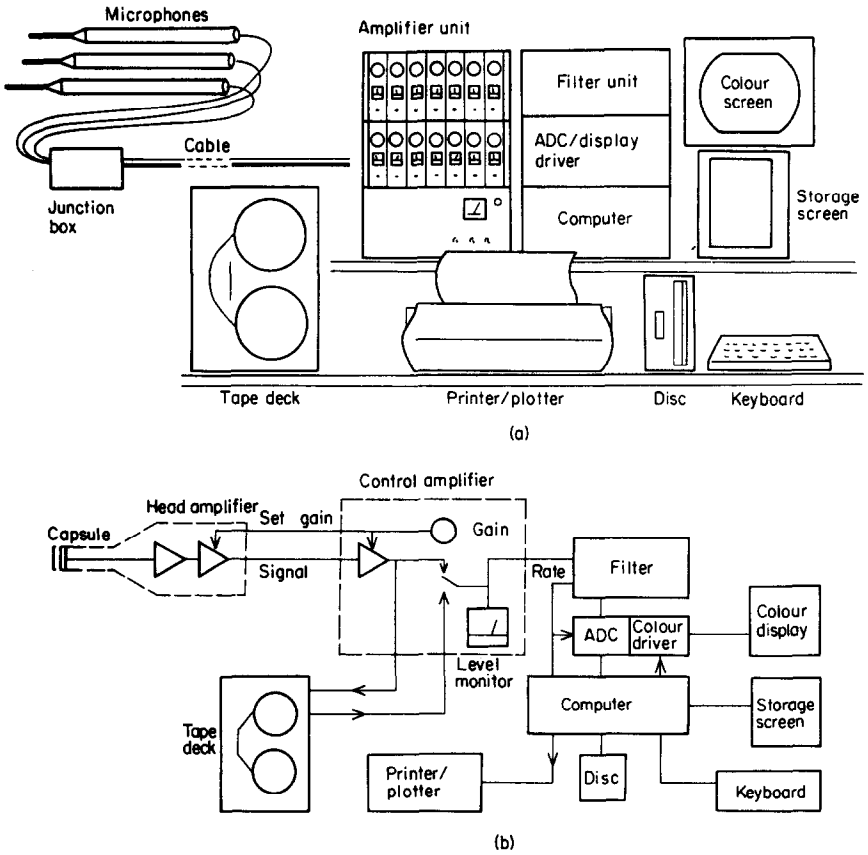

Figure 1. The telescope. (a) Physical; (b) schematic.

signals are converted to digital form. They are sampled in pairs at 6 μs intervals and digitized to 8-bit precision. The spread of 36 μs over which sampling takes place will have the effect of imparting a slight "squint" to the telescope. This is invariably less than 0·2° in angle for tests on full-size engines and since the telescope is always calibrated by using a loudspeaker source at known positions, it is doubly negligible. When sampling rates below the maximum are required, "burst-firing" is used, in which the channels are sampled in swift succession, with a dwell-time between each set of samples. "Squint" is then never worse than its minimum value.

The computer is a CAI LSI-2 with a memory capacity of 48 kilobytes. The analysis software is written within a FORTRAN framework, with calls to assembly language routines for time critical operations. It is discussed in a later section.

For backing store, the computer uses a "floppy-disc" system, with a capacity of 0·3 megabytes. This serves as program storage, and also allows data blocks to be stored, whether as raw sample values for further analysis or as computed results arrays. Control is via an electronic keyboard used in conjunction with a storage display screen. The screen has full graphic capabilities, and is one means of displaying the results. For hard copy, the system has a Diablo printer, capable of high-class typewriter standard printing, which is equally able to plot graphs to a resolution of about half a millimetre. To give an immediate impression of the results array, which contains intensity of source as a function of both frequency and position, a colour television display is used, where eight levels of sound intensity are represented by the colours: black, blue, red, magenta, green, cyan, yellow and white. The entire system is transportable, and can be carried in an estate car.

3. THE ANALYSIS TECHNIQUE

Consider first a block of, say, 512 sets of samples, having been digitized at 20 kHz per channel and stored in computer memory. Although these will occupy a continuous succession of storage locations, they may be imagined as an array fourteen columns wide, 512 rows long. In each row are fourteen values of signal, one from each microphone, all digitized "simultaneously". Each succeeding row contains signals logged 50 μs later than its predecessor; each column contains a time-series for the corresponding microphone signal.

Now consider a single event, causing an impulse of sound centred somewhere in front of the microphone array. The event will produce a spherical wavefront which will strike the microphones at differing instants, depending on the distance of each from the event. In order to simplify this discussion of the data processing technique, suppose that the sound

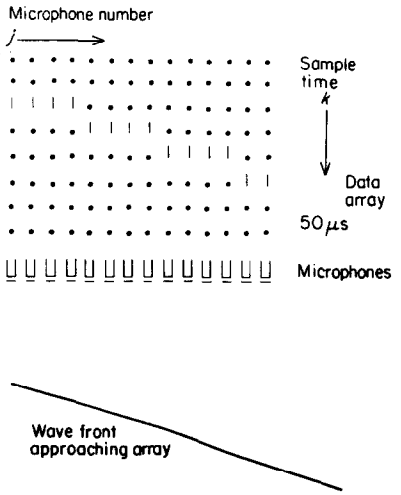

Figure 2. Simplified illustration of the effect of a single event on the data array.

source is remote from the array so that the curvature of the wavefront can be neglected. When the resulting signals are logged each microphone time series will (ideally) contain a single entry influenced by the event. When the data array is viewed as a whole, entries influenced by the event will form an approximately linear "wavefront" within the matrix. An illustration is given in Figure 2.

Let an element of the data array be represented as $s(k, j)$, this being the sample logged for the jth microphone at time $k\tau$ ($\tau = 50$ μs) (a list of notation is given in the Appendix). Suppose that the wavefront entries are $s(K_1, 1)$, $s(K_2, 2) \ldots s(K_{14}, 14)$ and that these have value 1 whilst all the other entries are zero. If the location of the event is known, the relative values of K_1 to K_{14} can be computed.

If one now constructs the time series $S_0(k) = \sum_{j=1}^{14} s(k + K_j, j)$ one sees that it has zero value for k negative or greater than zero, whilst $S_0(0)$ has the value 14 (the number of channels). One is summing the channel samples over a similar wavefront, displaced k units in time. When this corresponds to the actual wavefront, a large output is obtained as shown in Figure 3(a).

Now one can "tilt" the summation wavefront by adding j to each channel sample number, to form the telescope signal $S_1(k) = \sum_{j=1}^{14} s(k + K_j + j, j)$. When $k = -1$, S_1 will gain a unit contribution from channel 1, but zero from the rest. When $k = -2$, S_1 will gain a unit contribution from channel 2, but zero from the rest and so on. Thus, $S_1(k)$ has the form shown in Figure 3(b). It takes the value 1 for $-14 \leqslant k \leqslant -1$, but is otherwise zero. On this basis the next tilt angle would be obtained by adding $2j$ to the reference time series index, and so on. This

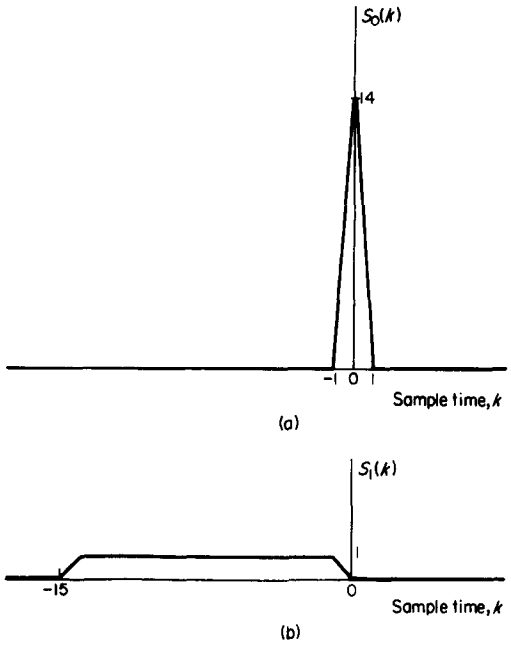

Figure 3. The summed signal $S(k)$: (a) "on target" and (b) "tilted".

may correspond to excessively large steps in the tilt angle and in practice, smaller increments are introduced by combining those data which are sampled closest to the exact time base requirements for each angle selected. Indeed, the step structure of the wavefront entries in the data array shown in Figure 2 is associated with sampling "jitter", giving a maximum error of ± 25 μs.

If one searches for the source by evaluating $\sum_k (S_n(k))^2$ where $S_n(k) = \sum_{j=1}^{14} s(k + K_j + nj, j)$ over a block of data, one will obtain a maximum value of 14^2 when $n = 0$, but only 14 when n takes any other integral value.

The angle of tilt away from the propagation direction of the intercepted wavefront when $n = 1$ is roughly 1·5° for a 3·9 metre telescope, or 0·75° for a 7·8 metre telescope. This very empirical analysis suggests a broad-band discrimination function of the form shown in Figure 4.

Of course, once the time series $S_n(k)$ has been constructed, much more can be done with it than this simple power calculation. Frequency-related data may be extracted by first performing a Fourier transform on the signal, and then perhaps accumulating the power over tenth-

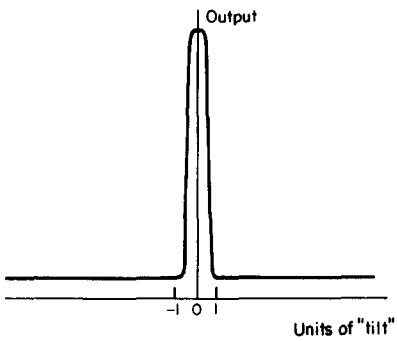

Figure 4. Empirical discrimination function for a "white noise" source. A "tilt unit" is 0·75° for a 7·8 m array and a sampling interval of 50 μs.

decade (i.e., third-octave) ranges. The resolution function will no longer be as in Figure 4, but will now depend on each frequency range. When the frequency bands chosen are narrow, positional "aliases" can occur for the high frequencies corresponding to a "tilt" of one or more complete wavelengths per microphone separation. Nevertheless, much useful information can be extracted in a few seconds from a relatively short sound sample.

Analysis need not be restricted to simple additive processing. Instead of summing the samples on a "wavefront", cross-products of partial sums of these selected samples may be used. A development of the procedure for frequency domain application has been described by Flynn and Kinns [8].

A further analysis technique uses a moving focus. Present methods of analysis average the sound over each part of the jet axis, akin to taking a photographic time-exposure. If the "tilt" of the analysis wavefront is increased progressively as it moves down the array, i.e. $S(k) = \sum_{j=1}^{14} s(k + K_j + \alpha_j k, j)$, then the focal point will move with time along the jet axis with velocity proportional to α. There is no physical limit on the effective speed of this tracking, and so moving features of the jet distribution could be frozen, akin to swinging a photographic camera to capture a moving subject. Of course noise levels would be high since integration times are limited to the time-of-flight of a feature within the jet. However, a type of data may be gained this way which appears impossible to obtain by any other method. Results of such analysis are to be reported separately.

The informal approach of this section has indicated some ways in which the array of microphones might be used to deduce the position or the position/time history of an unknown sound source as it appears from the far field. The simplest approach to sound source location utilizes additive processing and a detailed frequency domain analysis is presented in the next section. Here, a line source of correlated monopoles is used as a model for the sound source. It shares the far field properties of a jet engine noise source and allows arbitrary directionality through the correlation of component sources. However, these component sources need not be omni-directional. For example it is possible to assign the directionality of the resultant radiated field to each of them, through non-uniform weighting of microphone signals according to the measured field shape at each frequency. The analysis is extended to the cases where microphones are used in a moving airstream. The expected magnitude of statistical variations with respect to data sample length and the influence of atmospheric turbulence are also described briefly.

In these theoretical studies, the microphone signals are treated as continuous in order to simplify the analysis. The use of data which are sampled closest to the required time instants, in forming the sampled signal for a specified focus, has been found to cause negligible degradation of performance for frequencies up to a quarter of the data sampling rate.

4. THEORETICAL CONSIDERATIONS

4.1. THEORY FOR A LINE SOURCE OF SOUND RADIATORS

Figure 5 shows the acoustic array consisting of a line of N microphones, distance d from a line source. Let the instantaneous line source density be $q(y, t)$ and allow arbitrary correlation between sources. The mathematical model used in this section was chosen for its simplicity and tractability, and is similar to that used by Kinns [3] and Flynn and Kinns [8]. Although a line array of microphones has been preferred for ease of alignment, similar analysis is easily developed for other array configurations.

In the linear source analogy, the acoustic environment is ideal, the speed of sound c is constant, there are no undesired reflections, and the microphones are ideal point receivers.

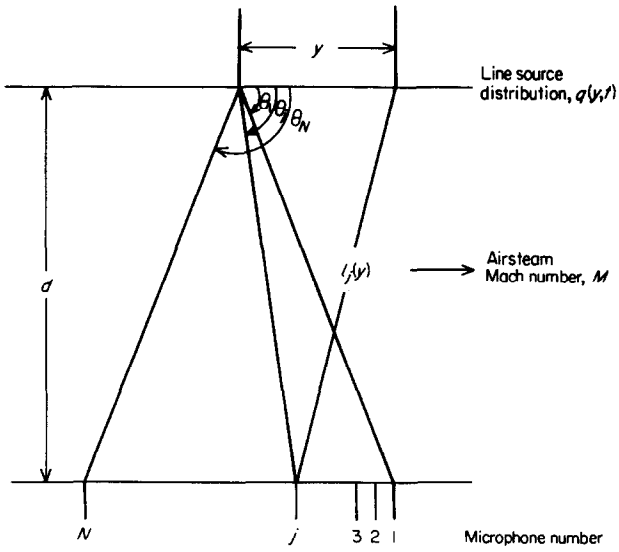

Figure 5. Diagram for theory.

The signal received at the jth microphone in Figure 1 is given by

$$p_j(t) = \int_{-\infty}^{\infty} \frac{q\left(y, t - \dfrac{l_j(y)}{c}\right)}{l_j(y)} \mathrm{d}y, \tag{1}$$

where $l_j(y)$ is the distance from the assumed source at y to the jth microphone. If the array is focused at a position y_0 on the line of sources, so that each signal is delayed by T_j and weighted by w_j before summation, the following signal is obtained from the microphone array:

$$S(y_0, t) = \sum_{j=1}^{N} p_j(t + T_j) w_j, \tag{2}$$

where

$$T_j = l_j(y_0)/c. \tag{3}$$

The weights w_j can be written as

$$w_j = w_{0j}\, l_j(y_0), \tag{4}$$

where the w_{0j} are independent of focal position and are used to vary the characteristics of the spatial window for a given array configuration.

Thus, the telescope signal can be written as

$$S(y_0, t) = \sum_{j=1}^{N} \int_{-\infty}^{\infty} w_{0j} \frac{l_j(y_0)}{l_j(y)} q\left(y, t + \frac{l_j(y_0) - l_j(y)}{c}\right) \mathrm{d}y. \tag{5}$$

Its Fourier transform is

$$G(y_0, f) = \int_{-\infty}^{\infty} S(y_0, t)\, \mathrm{e}^{-2\pi \mathrm{i} f t} \mathrm{d}t = \sum_{j=1}^{N} w_{0j} \int\int_{-\infty}^{\infty} q(y, t') \frac{l_j(y_0)}{l_j(y)} \mathrm{e}^{-2\pi \mathrm{i} f t'}\, \mathrm{e}^{(2\pi \mathrm{i}/\lambda)(l_j(y_0) - l_j(y))} \mathrm{d}y\, \mathrm{d}t', \tag{6}$$

where λ is the wavelength of sound at frequency f, so that

$$G(y_0,f)=\int_{-\infty}^{\infty} Q(y,f)\left\{\sum_{j=1}^{N} w_{0j}\frac{l_j(y_0)}{l_j(y)}e^{(2\pi i/\lambda)(l_j(y_0)-l_j(y))}\right\}dy, \tag{7}$$

where

$$Q(y,f)=\int_{-\infty}^{\infty} q(y,t)\,e^{-2\pi i f t}\,dt \tag{8}$$

is the Fourier transform of the source density. It follows at once that if the source region is statistically stationary in time the power spectral density of the telescope signal for focal position y_0 and frequency f is given by

$$P_{ss}(y_0,f)=\int_{-\infty}^{\infty}\int Q_{yy'}(f)\left[\sum_{j=1}^{N} w_{0j}\frac{l_j(y_0)}{l_j(y)}e^{(-2\pi i/\lambda)(l_j(y_0)-l_j(y))}\right]\times$$

$$\times\left[\sum_{j=1}^{N} w_{0j}\frac{l_j(y_0)}{l_j(y')}e^{(2\pi i/\lambda)(l_j(y_0)-l_j(y'))}\right]dy\,dy', \tag{9}$$

where

$$Q_{yy'}(f)=\int_{-\infty}^{\infty}\mathrm{Ex}\,[q(y,t)q(y',t+\tau)]e^{-2\pi i f\tau}d\tau \tag{10}$$

is the cross-spectrum of source densities at y and y'.

Equation (9) is the general double integral relationship between the power spectral density of the telescope signal for a specified focus and the cross-spectrum of source density components. However, the path length $l_j(y)$ is given by

$$l_j(y)=d\,\mathrm{cosec}\,\theta_j\left\{1+\left[\left(\frac{y\sin\theta_j}{d}\right)^2-\frac{y}{d}\sin 2\theta_j\right]\right\}^{1/2}, \tag{11}$$

and a second order expansion in y/d can be used to demonstrate the essential properties of equation (9).

4.2. THEORY TO SECOND ORDER IN y/d

To second order in y/d and with inclusion of contributions from both first and second powers of the term in square brackets in equation (11)

$$l_j(y)=d\,\mathrm{cosec}\,\theta_j\left\{1+\frac{y^2\sin^4\theta_j}{2d^2}-\frac{y\sin\theta_j\cos\theta_j}{d}\right\}, \tag{12}$$

so that

$$l_j(y_0)-l_j(y)\approx\frac{y_0^2-y^2}{2d}-(y_0-y)\left\{\left(\frac{y_0+y}{2d}\right)(1-\sin^3\theta_j)+\cos\theta_j\right\}. \tag{13}$$

If $(y_0+y)/2d$ is small and θ_j is close to $\pi/2$, equation (13) can be simplified to

$$l_j(y_0)-l_j(y)=(y_0^2-y^2)/2d-(y_0-y)\cos\theta_j, \tag{14}$$

while $l_j(y_0)/l_j(y)=1$, to first order in y/d.

With the above approximations, equation (9) can be written as

$$P_{ss}(y_0,f) = \int_{-\infty}^{\infty}\int Q_{yy'}(f)\,e^{(-2\pi i/\lambda)[(y'^2-y^2)/2d]}\left[\sum_{j=1}^{N} w_{0j}\,e^{(-2\pi i/\lambda)(y_0-y)\cos\theta_j}\right]\times$$

$$\times\left[\sum_{j=1}^{N} w_{0j}\,e^{(2\pi i/\lambda)(y_0-y')\cos\theta_j}\right]dy\,dy'. \tag{15}$$

One can define a modified cross-spectrum of source densities,

$$Q'_{yy'}(f) = Q_{yy'}(f)\,e^{(-2\pi i/\lambda)[(y'^2-y^2)/2d]}, \tag{16}$$

so that equation (15) takes the same form regardless of distance from the source. The modification of the cross-spectrum corresponds to the second order dependence of apparent source intensity on the position of the array centre, through the directivity of the source region resulting from correlation of component sources. This problem in source location was discussed by Kinns [3]. The phase factor in equation (16) may be important, even where $\pi(y'^2 - y^2)/\lambda d \ll 1$, since closely spaced sources may be nearly self-cancelling.

A familiar basis for comparison is provided by setting the weights w_{0j} to unity and using a microphone spacing policy such that

$$\cos\theta_j = \cos\theta_1 - (j-1)\,\Delta \tag{17}$$

and

$$\cos\theta_1 = -\cos\theta_N = (N-1)\,\Delta/2. \tag{18}$$

Then, equation (15) can be written as

$$P_{ss}(y_0,f) = \int_{-\infty}^{\infty}\int \frac{Q'_{yy'}(f)\sin\dfrac{N\pi\Delta}{\lambda}(y_0-y)\sin\dfrac{N\pi\Delta}{\lambda}(y_0-y')}{\sin\dfrac{\pi\Delta}{\lambda}(y_0-y)\sin\dfrac{\pi\Delta}{\lambda}(y_0-y')}\,dy\,dy'. \tag{19}$$

Each multiplying factor of the form

$$\left\{\sin\frac{N\pi\Delta}{\lambda}(y_0-y)\right\}\Big/\left\{\sin\frac{\pi\Delta}{\lambda}(y_0-y)\right\} \tag{20}$$

tends to the Dirac delta function $\delta(y_0 - y)$ as Δ/λ tends to zero and $N\Delta/\lambda$ tends to infinity. If that limit could be approached, the telescope would allow the power spectral density of the source at focal position y_0, $Q'_{y_0y_0}(f) = Q_{y_0y_0}(f)$, to be determined. Similarly, it would be possible to determine the cross-spectral density of source components at any two focal positions and this can be regarded as the limiting capability of the telescope. However, the aperture of the telescope, $\theta_N - \theta_1$, is restricted to 180°, the number of microphones is limited, and the wavelength is determined by the frequency. Indeed, the cross-spectrum of source components $Q_{yy'}(f)$ may tend to zero with increasing $(y - y')$ more rapidly than the multiplying factors (20) with $(y_0 - y)$ and $(y_0 - y')$. In order to explore this situation further, equation (19) may be written as

$$P_{ss}(y_0,f) = \int_{-\infty}^{\infty}\int \mathrm{Re}\,[Q'_{yy'}(f)]\left\{\frac{\sin\left(\dfrac{N\pi\Delta}{\lambda}(y_0-y)\right)\sin\left(\dfrac{N\pi\Delta}{\lambda}((y_0-y)+(y-y'))\right)}{\sin\left(\dfrac{\pi\Delta}{\lambda}(y_0-y)\right)\sin\left(\dfrac{\pi\Delta}{\lambda}((y_0-y)+(y-y'))\right)}\right\}dy'\,dy. \tag{21}$$

It can be seen that providing $\mathrm{Re}[Q'_{yy'}(f)]$ is only significant for spacings of y and y' such that $|y-y'| \ll \lambda/N\Delta$ and is not violently oscillatory in that range, equation (21) can be approximated by

$$P_{ss}(y_0,f) \approx \int_{-\infty}^{\infty}\int \mathrm{Re}[Q'_{yy'}(f)] \frac{\sin^2 \dfrac{N\pi\Delta}{\lambda}(y_0-y)}{\sin^2 \dfrac{\pi\Delta}{\lambda}(y_0-y)} \mathrm{d}y'\,\mathrm{d}y. \tag{22}$$

Furthermore, one can define an effective source intensity [3] as

$$\bar{R}'(y,f) = \int_{-\infty}^{\infty} \mathrm{Re}[Q'_{yy'}(f)]\,\mathrm{d}y', \tag{23}$$

which allows equation (22) to be reduced to a single integral:

$$P_{ss}(y_0,f) \approx \int_{-\infty}^{\infty} \bar{R}'(y,f) \frac{\sin^2 \dfrac{N\pi\Delta}{\lambda}(y_0-y)}{\sin^2 \dfrac{\pi\Delta}{\lambda}(y_0-y)} \mathrm{d}y. \tag{24}$$

This approximation is appropriate to the small aperture telescope where the resolving power is insufficient to separate the correlated components of the equivalent line source and where the directionality of the source region does not lead to large changes in signal intensity across the microphone array. It is exact when the component sources are uncorrelated [8].

The effect of directionality can be explored by redefining the source distribution so that each component has the directionality of the resultant field, but may still be correlated with other components. Rather than set the weights w_{0j} to unity, one would then set them according to the measured directionality at each frequency and obtain a different expression for the relation between the power spectrum of the (new) telescope signal and the source properties. However, weighting of the microphone signals according to position is equivalent to application of a non-uniform data window in time series analysis and its effect on the multiplying factors given by equation (20) is readily computed. It should be noted that the weighting function derived in this way tends more closely to the rectangular, and equation (21) is better approximated by equation (22), as the aperture is reduced.

Equation (24) can be written in the form

$$P_{ss}(y_0,f) = \int_{-\infty}^{\infty} \bar{R}'(y,f)\, C_0\left(\frac{y_0-y}{\lambda}\right)\mathrm{d}y, \tag{25}$$

where

$$C_0\left(\frac{y_0-y}{\lambda}\right) = \left\{\sin^2\left(\frac{N\pi\Delta}{\lambda}(y_0-y)\right)\right\} \Big/ \left\{\sin^2\left(\frac{\pi\Delta}{\lambda}(y_0-y)\right)\right\} \tag{26}$$

is a special case of a frequency dependent spatial window. In general, it is desirable to choose the number of microphones, their position and the weights w_{0j} to give a spatial window with a maximum at $(y_0-y)=0$ and a rapid decay with increasing (y_0-y).

The form of C_0 is presented as a function of $\pi\Delta(y_0-y)/\lambda$ in Figure 6 for the case $N=14$. It has a main lobe with a half-power width of approximately

$$0{\cdot}45\left(\frac{N-1}{N}\right)\frac{\lambda}{\cos\theta_1} \approx 0{\cdot}063\frac{\lambda}{\Delta} \qquad \text{when } N=14. \tag{27}$$

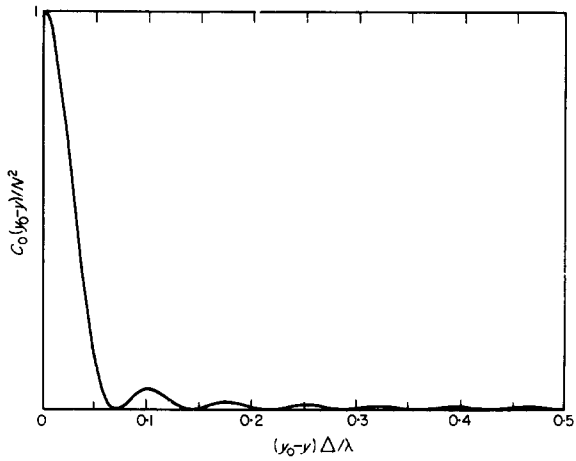

Figure 6. Basic convolution window for uncorrelated monopoles for additive processing with $N = 14$ microphones.

It is also cyclic in $(y_0 - y)$ and the spacing of successive maxima is

$$\lambda(N-1)/2\cos\theta_1 = \lambda/\Delta. \tag{28}$$

If the number of microphones is fixed, a reduction in the aperture increases the spacing of successive maxima, or aliases, in the same proportion as the half-power bandwidth which governs the extent to which separated sources can be resolved. The frequency dependence of the spatial resolving power may mean that the spacing of microphones has to be varied according to the frequency range under investigation. One of the main advantages of an on-line analysis system is that microphone positions can be varied according to observed results, for optimum use of a relatively small number of microphones.

The use of $w_{0j} = 1$ requires the weighting of microphone signals according to their position in the array and it is simpler in practice to use uniform weighting, with straightforward adjustment for small differences in gain between microphones. The weights w_{0j} can then be approximated by $w_{0j} = \sin\theta_j$, since a first order approximation to the source to microphone distance is $d\operatorname{cosec}\theta_j$ from Figure 5. The effect of these weighting terms is small when θ_j is close to $\pi/2$, but they do have a significant effect when the aperture of the array $(\theta_N - \theta_1)$ increases beyond 30° or so. In particular, they lead to an appreciable reduction in the amplitudes of the sidelobes shown in Figure 6.

Although the choice of equal spacing in $(\cos\theta_j)$ is amenable to analysis, the use of equal microphone spacing is simplest for field application. At angular apertures less than about 20° the differences are small, but at large apertures, the cyclic properties of the spatial window given by equation (26) are no longer obvious when equal microphone spacing is used. In order to illustrate this, Figure 7 shows a comparison of $C_1([y_0 - y]/\lambda)$ for equal cosine spacing and weighting of microphone signals, with $C_2([y_0 - y]/\lambda)$ for equal spacing of microphones and weighting of signals, for the same aperture of 60°.

The distortion of aliases, shown by Figure 7 for equal microphone spacing, can make interpretation difficult where the source scale is of the same order as the spacing of aliases. However, repetition of aliases with equal cosine spacing will only occur where the approximations in the derivation of equation (15) are valid. This will be the case where the spacing of aliases is much smaller than the distance between source region and microphones. Nevertheless, the slight additional complexity of equal cosine spacing is justifiable for ease of interpretation at high frequencies.

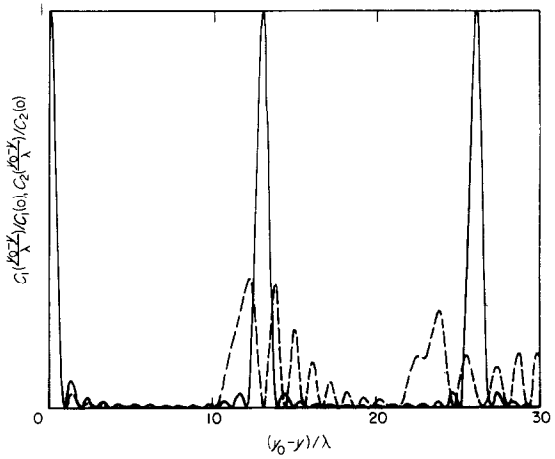

Figure 7. Apparent distributions for a monopole source when using additive processing and 14 microphones with an aperture of 60° and two spacing policies. ——, Equal cosine spacing, C_1; ---, equal spacing, C_2.

The weights w_{0j} can be varied without difficulty, by using a digital processor, so that a suitable compromise between half-power width of the main lobe of the spatial window and the magnitude of the side lobes can be found. However, there are other techniques for modifying the form of the spatial window which allow greater variations. These include frequency domain multiplicative processing [8].

Although the double convolution integral (equation (19)) must be recognized in a general study, the reduction to a single integral in equation (24) makes it an attractive basis for initial interpretation of $P_{ss}(y_0,f)$ with respect to focal position y_0, especially as the cross-spectra for different focal positions can be computed directly (q.v.).

4.3. A SIMPLIFIED ANALYSIS OF THE INFLUENCE OF GROUND REFLECTIONS

In practical engine applications, it is necessary to accept the existence of ground reflections, where the surface is usually flat concrete. Strictly, an analysis of the ground reflections problem should include recognition of the relatively large thickness of an exhaust jet in relation to its height above the ground, and the imperfect reflective qualities of the ground surface. Nevertheless a clear idea of the nature of the problem can be gained by assuming that the ground is a perfect reflector so that there is no attenuation or phase shifting of sound on reflection, and that the source region can be approximated by a line source as above.

Figure 8 shows a test situation in which a source of sound is positioned h_1 above the reflecting surface, with the microphone positioned h_2 above the surface. Let the direct path be $l(y)$ as before. Then, the reflected path $r(y)$ is given by:

$$r^2(y) = l^2(y) + 4h_1 h_2. \tag{29}$$

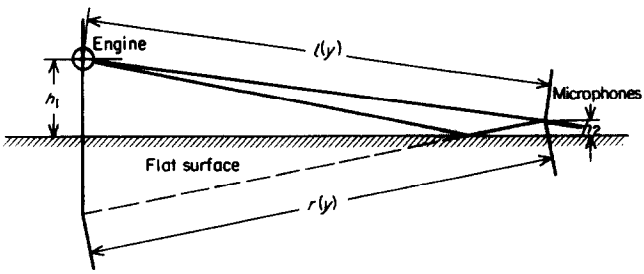

Figure 8. Diagram for studies of ground reflections.

In place of equation (1) one then has

$$p_j(t) = \int_{-\infty}^{\infty} \frac{1}{l_j(y)} q\left(y, t - \frac{l_j(y)}{c}\right) + \frac{1}{r_j(y)} q\left(y, t - \frac{r_j(y)}{c}\right) \mathrm{d}y \tag{30}$$

for the combined influences of direct and reflected rays. In practical test situations $4h_1h_2/l^2(y) \ll 1$, so that the amplitudes of direct and reflected waves are almost equal and the main effect stems from an effective time delay between their arrivals at the microphone. Equation (30) can therefore be simplified to

$$p_j(t) \approx \int_{-\infty}^{\infty} \frac{1}{l_j(y)} \left[q\left(y, t - \frac{l_j(y)}{c}\right) + q\left(y, t - \frac{l_j(y) + \dfrac{2h_1h_2}{l_j(y)}}{c}\right)\right] \mathrm{d}y. \tag{31}$$

The telescope signal is formed for a specified focus, by using equation (2) as before, but with modified time delays T' which compensate for the influence of ground reflections as follows:

$$T_j' = \{l_j(y_0) + \delta_j(y_0)\}/c, \tag{32}$$

where

$$\delta_j(y_0) = h_1h_2/l_j(y_0). \tag{33}$$

The telescope signal for focus y_0 is then given by

$$S(y_0,t) = \sum_{j=1}^{N} \int_{-\infty}^{\infty} w_{0j} \frac{l_j(y_0)}{l_j(y)} \left\{ \begin{array}{l} q\left(y, t + \dfrac{l_j(y_0) - l_j(y) + \delta_j(y_0)}{c}\right) \\ + q\left(y, t + \dfrac{l_j(y_0) - l_j(y) + \delta_j(y_0) - 2\delta_j(y)}{c}\right) \end{array} \right\} \mathrm{d}y. \tag{34}$$

Its Fourier transform is

$$G(y_0,f) = \int_{-\infty}^{\infty} Q(y,f) \left\{ 2 \sum_{j=1}^{N} w_{0j} \frac{l_j(y_0)}{l_j(y)} \cos\left(\frac{2\pi\delta_j(y)}{\lambda}\right) \mathrm{e}^{(2\pi\mathrm{i}/\lambda)(l_j(y_0)+\delta_j(y_0)-l_j(y)-\delta_j(y))} \right\} \mathrm{d}y. \tag{35}$$

which can be simplified to

$$G(y_0,f) = \int_{-\infty}^{\infty} Q(y,f) \left\{ 2 \sum_{j=1}^{N} w_{0j} \cos\left(\frac{2\pi\delta_j(y)}{\lambda}\right) \mathrm{e}^{(2\pi\mathrm{i}/\lambda)(y_0-y)(1-[h_1h_2/l_j^2(y_0)])\cos\theta_j} \right\} \mathrm{d}y, \tag{36}$$

by using the approximations leading to equations (15) and (33).

Providing $\cos(2\pi\delta_j(y)/\lambda)$ is approximately the same for all significant values of y, the influence of ground reflections is just to cause a modulation of apparent source strength with respect to frequency. The factor $(1 - h_1h_2/l_j^2(y_0))$ which modifies the phase, causes a negligible broadening of the convolution window, since $h_1h_2/l_j^2(y_0) \ll 1$ for typical values of h_1, h_2 and $l_j(y_0)$. Variations in $\cos(2\pi\delta_j(y)/\lambda)$ with respect to j will tend to be small when this factor is close to unity, since its rate of change with respect to $\delta_j(y)$ is then a minimum. When the aperture is small, little deterioration in resolving power is expected away from wavelengths which lead to near cancellation of direct and reflected sound waves at any of the microphones. This was confirmed by results from tests on a Rolls-Royce Viper engine [7], with an array aperture of about 15° and high level microphones.

4.4. THEORY FOR MEASUREMENTS IN A WIND TUNNEL

One of the outstanding problems in noise research is to identify the influence of forward motion on turbojet engine noise sources. In this section, a procedure for processing of signals when a moving airstream is placed between the source region and the array of microphones, is described. The mathematical model for the source region is a line of correlated sound sources which radiate into the moving stream with omnidirectional sound pressure. The direction of the airstream with Mach number M is indicated in Figure 5.

The effective path length between a source at y and the jth microphone is now given by

$$l_j(y) = \frac{d\,\mathrm{cosec}\,\theta_j}{1-M^2}\left\{M\left(\frac{y\sin\theta_j}{d} - \cos\theta_j\right) + \left[1 + \frac{y^2}{d^2}\sin^2\theta_j - \frac{y}{d}\sin 2\theta_j - M^2\sin^2\theta_j\right]^{1/2}\right\}, \quad (37)$$

which reduces to equation (11) when $M = 0$. In practice, the Mach number M is less than 0·3 and a second order expansion in M and y/d gives

$$l_j(y_0) - l_j(y) \approx \frac{y_0^2 - y^2}{2d} - (y_0 - y)\left\{\left(\frac{y_0 + y}{2d}\right)(1 - \sin^3\theta_j) + (\cos\theta_j - M)\right\}. \quad (38)$$

By using the approximation of equation (14) and the modified cross-spectrum defined by equation (16), it can be shown that

$$P_{ss}(y_0, f) = \int_{-\infty}^{\infty}\int Q'_{yy'}(f)\,e^{[-2\pi i(y'-y)M/\lambda]}\left\{\sum_{j=1}^{N} w_{0j}\,e^{(2\pi i/\lambda)(y_0-y)\cos\theta_j}\right.$$

$$\left.\times \sum_{j=1}^{N} w_{0j}\,e^{(-2\pi i/\lambda)(y_0-y')\cos\theta_j}\right\} dy\,dy', \quad (39)$$

which is identical to equation (15) apart from the phase factor containing the Mach number. This factor corresponds to an upstream shift of the array in the static case, equivalent to the change in direction of sound waves due to the moving airstream.

This analysis shows how it is only necessary to modify the set of time delays corresponding to each focal position for the telescope to be used in a moving airstream with correct identification of source position. The software modification is trivial and the computer system performance is sufficient to allow compensation for wind speed fluctuations according to the signal from a transducer.

4.5. THE CROSS-CORRELATION OF SIGNALS FROM DIFFERENT TELESCOPE FOCI

One of the most useful facilities of a digital processer is the ease with which analysis can be extended beyond routine estimation of sound source intensity with respect to axial position. It is scarcely more difficult to correlate signals from two foci than to study the properties of the telescope signal for a single focus. This gives the combination of an array of microphones and a digital processer a huge advantage over techniques which must be restricted to one type of analysis.

In this section the cross-spectrum of signals from two foci are considered. The telescope signals are formed by summation of time-lagged microphone signals as before, and are given by

$$S(y_0, t) = \sum_{j=1}^{N}\int_{-\infty}^{\infty} w_{0j}\,\frac{l_j(y_0)}{l_j(y)}\,q\left(y, t + \frac{l_j(y_0) - l_j(y)}{c}\right) dy \quad (40)$$

and

$$S'(y_0', t) = \sum_{j=1}^{N} \int_{-\infty}^{\infty} w_{0j} \frac{l_j(y_0')}{l_j(y')} q\left(y', t + \frac{l_j(y_0') - l_j(y')}{c}\right) \mathrm{d}y'. \tag{41}$$

It follows that the cross-spectrum of the signals can be written as

$$P_{ss'}(y_0, y_0', f) = \int\int_{-\infty}^{\infty} Q_{yy'}(f) \left[\sum_{j=1}^{N} w_{0j} \frac{l_j(y_0)}{l_j(y)} \mathrm{e}^{(-2\pi \mathrm{i}/\lambda)(l_j(y_0) - l_j(y))}\right] \times$$

$$\times \left[\sum_{j=1}^{N} w_{0j} \frac{l_j(y_0')}{l_j(y')} \mathrm{e}^{(2\pi \mathrm{i}/\lambda)(l_j(y_0') - l_j(y'))}\right] \mathrm{d}y\, \mathrm{d}y', \tag{42}$$

which is the equivalent of equation (9) for the power spectrum. The equivalent result to equation (15) is

$$P_{ss'}(y_0, y_0', f) = \int\int_{-\infty}^{\infty} Q_{yy'}(f)\, \mathrm{e}^{(-\pi \mathrm{i}/\lambda d)(y_0^2 - y_0'^2 + y'^2 - y^2)} \left[\sum_{j=1}^{N} w_{0j}\, \mathrm{e}^{(2\pi \mathrm{i}/\lambda)(y_0 - y)\cos\theta_j}\right] \times$$

$$\times \left[\sum_{j=1}^{N} w_{0j}\, \mathrm{e}^{(-2\pi \mathrm{i}/\lambda)(y_0' - y')\cos\theta_j}\right] \mathrm{d}y\, \mathrm{d}y'. \tag{43}$$

The assumption of equal cosine spacing (equations (17) and (18)) and $w_{0j} = 1$ then gives

$$P_{ss'}(y_0, y_0', f) = \int\int_{-\infty}^{\infty} Q_{yy'}(f)\, \mathrm{e}^{(-\pi \mathrm{i}/\lambda d)(y_0^2 - y_0'^2 + y'^2 - y^2)} \frac{\sin\dfrac{N\pi\Delta}{\lambda}(y_0 - y) \sin\dfrac{N\pi\Delta}{\lambda}(y_0' - y')}{\sin\dfrac{\pi\Delta}{\lambda}(y_0 - y) \sin\dfrac{\pi\Delta}{\lambda}(y_0' - y')} \mathrm{d}y\, \mathrm{d}y'. \tag{44}$$

Thus, to limited resolution, the array of microphones can be used to estimate the properties of $Q_{yy'}(f)$ for various y and y' corresponding to y_0 and y_0'.

Finally, the case where sources are uncorrelated with respect to axial position gives

$$\bar{P}_{ss'}(y_0, y_0', f) = \int_{-\infty}^{\infty} \bar{Q}(y, f)\, \mathrm{e}^{(-\pi \mathrm{i}/\lambda d)(y_0^2 - y_0'^2)} \frac{\sin\dfrac{N\pi\Delta}{\lambda}(y_0 - y) \sin\dfrac{N\pi\Delta}{\lambda}(y_0' - y)}{\sin\dfrac{\pi\Delta}{\lambda}(y_0 - y) \sin\dfrac{\pi\Delta}{\lambda}(y_0' - y)} \mathrm{d}y, \tag{45}$$

since $Q_{yy'}(f) = \bar{Q}(y, f)\delta(y - y')$ for the case of uncorrelated sources.

In this case, the cross-spectrum of array signals is governed by the resolving power of the array and remains large over a range corresponding to the width of the main lobe shown in Figure 6. Usually, it is possible to make useful measurements of the cross-spectrum only for separations of y_0 and y_0' which exceed this range, and where the coherence of telescope signals is high.

4.6. STATISTICAL STABILITY OF TELESCOPE ESTIMATES

If the array of microphones is being used to estimate the expected value of source intensity at a specified location, it is important to be able to estimate the degree of reliability of measurements from finite data samples. Little is known of the detailed statistics of sound generation by jet engines, but we have found a Gaussian model to be adequate for estimation of the variability of estimates of power spectral density of a single microphone signal.

If it is assumed that each microphone signal has Gaussian properties, the sum of the lagged microphone signals must also be Gaussian, regardless of the correlation between these signals. Thus, confidence limits for source intensity estimates can be formulated in exactly the same way as for a single signal. The power and cross-spectral density estimates are computed by using techniques [9] based on the method of Welch [10], so that the equivalent number of degrees of freedom, n_f, is simply twice the number of independent data segments times a factor depending on the procedures for data modification and quadratic smoothing in the frequency domain. In the simplest analysis, where a uniform data window is used and segments are Fourier transformed without addition of zeros [10] or time domain aliasing [11], this factor is simply the number of adjacent estimates combined by quadratic smoothing, providing the spectral density is uniform.

The normalized standard error of spectral density estimates is

$$\sqrt{2}/n_f, \tag{46}$$

where the distribution of source intensity estimates obtained via the spectral density of the telescope signal for a fixed focus, is expected to be proportional to a chi-square distribution with n_f degrees of freedom.

Estimation of the coherence and phase of apparent sound sources at different positions is complicated by the dependence of errors on the true coherence as well as on n_f, but published results [12, 13] for the distribution of errors in estimates of phase, coherence and cross-spectra can be applied directly.

A series of tests to check the validity of the above criteria for the estimation of statistical errors was conducted by Kinns [14] on noise measurements from a Rolls-Royce/SNECMA Olympus engine. Analyses were performed on independent data samples with the engine running at various conditions from idle to full-power. The level of reproducibility of results was in good agreement with the above model.

4.7. THE INFLUENCE OF ENVIRONMENTAL DEFECTS

Although the theory indicates that the microphones should be as far away from the source region as possible, there are various practical limitations which restrict the usefulness of measurements a long way from the source. Reflections from remote objects and other sources of extraneous noise become more significant, while wind and temperature gradients, atmospheric absorption and ground roughness all tend to become more important with increasing propagation distance [15].

Clearly, the influence of atmospheric turbulence will vary according to the extent of the telescope array in relation to the size of atmospheric eddies. If all microphones lie within an eddy [16], variations in the slope of wave fronts will lead to an apparent width of a monopole source of order

$$ul^{3/2}\,e^{-1/2}/c, \tag{47}$$

where u is the r.m.s. turbulence velocity, c is the speed of sound, l is propagation distance and e is the eddy scale ($e < l$). Strictly, this formula is only applicable where $\lambda < e$. If the atmospheric variations are on such a scale that both source and microphones can be assumed to lie within a single eddy, the apparent width becomes

$$ul/c. \tag{48}$$

In both the above cases, the atmospheric fluctuations are assumed to be fully correlated across the microphones, but it may be more realistic to consider the wave drift at a single microphone as determining the degradation caused by atmospheric turbulence. This wave drift is of order

$$ul^{1/2}\,e^{1/2}/c, \tag{49}$$

and it can be seen that it is the largest eddies which are expected to have largest effect (cf. equation (47); also see reference [17]).

The appropriate compromise between the above three simple formulae is not easy to determine, owing to large uncertainties in the various parameters involved. In practice, calibration with a loudspeaker source at at least two known positions has been used to check the operation of the data processing system in prevailing conditions. It is in this uncertain situation that the ability to process signals on-line has particular value; microphone configurations can be altered for an effective compromise with minimum delay and expense.

5. SOFTWARE

5.1. THE SOFTWARE SYSTEM

Programs have been written to offer a diversity of analysis techniques. Data can be recorded in a "raw" form on flexible disc for subsequent analysis, or can be processed immediately after logging. Results arrays can be filed, or presented on either a colour television display or a storage display screen, or as a printed plot.

Before running the data processing program, an initialization program is run to set up a number of parameters and constants. This program interrogates the user to find such parameters as number and location of microphones, logging speed and required focal positions. It computes an array containing data shift parameters corresponding to the "wavefront" for each focus. The program also allows the user to specify the frequency range required and whether results are to be presented in constant bandwidth or 1/10 decade formats. It also computes the appropriate sine arrays and smoothing ranges to be used by the Fourier transform routines, after checking whether the user's requirements are compatible with the system design and guiding the user in any modification required. Parameters are stored in "Common" before they are used subsequently by the analysis program.

The routine for frequency domain analysis in which additive processing is used, corresponding to the theory of section 4, has been used most often. It first requires the user to identify the data source and destination. When used on-line, the data source is the analog-to-digital converter. To assist when setting-up, each channel may be displayed "live" on the screen. "Destination" may be disc, or analysis. In the latter case, blocks of data are analysed with the aid of sub-programs written in assembly-language for high speed processing.

A time series corresponding to each focal position is extracted from the data block. A periodogram is then obtained from this time series, by using a Fast Fourier Transform routine. The periodogram elements are then summed over specified frequency ranges and the contents of a results array are updated. This array can be displayed on the colour television to represent source intensities in up to 16 frequency bands and for up to 39 foci. The size of these ranges is largely a function of core-size (48 kilobytes in this case). The display sensitivity (dBs/colour step) can be chosen by the operator. The same results array can be displayed as a set of graphs on the storage-screen or can be plotted on the Diablo printer. It can also be put on to flexible-disc for subsequent presentation in any of these forms. The results array can be augmented or restarted, and the number of blocks to be analysed can be specified in advance.

Other analysis programs, including a corresponding routine for multiplicative processing [8] can be called by name from the disc system as required.

5.2. ANALYSIS TIME FOR ADDITIVE PROCESSING

The speed with which source distributions can be computed is governed largely by the number of microphones, N, the number of datum points per time series segment which are Fourier transformed for estimation of the power spectral density of the telescope signal, K, the number of data segments, n_s, and the number of foci, L. For simplicity K is restricted to

be an integral power of 2, but this is not a necessary constraint where a radix-2 Fast Fourier Transform algorithm is used [10, 11].

On the Computer Automation LSI-2/20 mini-computer the processing time is approximately $n_s LK(0{\cdot}050\log_2 K + 0{\cdot}016(N+3))$ milliseconds. Thus, if $L = 30$, $K = 256$ and $N = 14$, the execution time per segment is about 5 seconds for estimates at 129 frequencies.

Usually, a specified number of degrees of freedom n_f is required at a particular frequency in order to achieve appropriate statistical stability (see equation (46)). If the maximum resolution of order f_s/K is required, $n_f = 2n_s$ where f_s is the data sampling rate and it is assumed that data segments are independent of each other.

In order to condense data for storage and presentation, a 1/10 decade smoothing policy is commonly used. In that case, the following formula for n_f can be used for design purposes: $n_f = 0{\cdot}46Kn_s f_c/f_s$, where f_c is the centre frequency of the 1/10 decade of interest.

It is expected that further software refinement will lead to significant reductions in processing time, but the existing system has sufficient performance for direct field application.

6. EXPERIMENTS ON FULL-SIZE ENGINES

The results presented are typical of those obtained when using additive signal processing and demonstrate some of the characteristics of sound generation by full-size jet engines. The experiments on Rolls-Royce/SNECMA Olympus engines were performed with the help of the staffs of the Noise Departments at the Bristol Engines division of Rolls-Royce (1971) Limited, and of SNECMA.

These experiments were performed before the on-line system became available and some microphone signals were recorded, by using the 14-track Ampex FR1300A tape recorder with direct record electronics. Special replay amplifiers were constructed to allow reproduction of low frequency signals when tapes were replayed at $1\frac{7}{8}$ in/s. The reduced replay speed allowed a good match between data sampling and processing rates and thereby efficient utilization of the short recordings available. In later on-line experiments, higher sampling rates were used and any signal degradation due to tape recording could be avoided.

The television display format is used to illustrate the changes in the distribution of telescope signal intensity with respect to focal position and frequency which occur between low and high power conditions in the frequency range beyond 400 Hz, using a 12·5° telescope aperture. Output on the printer/plotter shows the changes which take place at frequencies from 100 Hz to 500 Hz, using a 30° aperture. A 1/10 decade presentation is used throughout.

In each experiment, the performance of the array was checked using a loudspeaker source with a width of about 0·6 metre. The microphone signals were given equal weighting, so that the w_{0j} in equation (4) showed a slight fall towards the ends of the array. However, this has a negligible effect for apertures less than 30°.

The analysis of section 4 showed that if the source region is represented by a line of arbitrarily correlated sound radiators, the basic property of the telescope is to allow the source intensity to be determined as a function of frequency and position, whether the equivalent line source exhibits spatial correlation or not. However, the limited aperture of the telescope means that the correlation of source components is likely to fall to small values within the width of the spatial window which defines the resolution capability. In terms of the same line source model, a study of the coherence between signals from closely spaced microphones [3, 18] for the same engine test conditions demonstrated that the equivalent line source components were not highly correlated at the extremes of the apparent source distribution represented by the variation of telescope signal spectral density with position. In particular, the properties of $\bar{R}'(y,f)$, derived from the observed results by using equation (24), were consistent with estimates of the root mean square extent of the distribution of $\bar{R}'(y,f)$ for the

case where component sources are not significantly correlated at separations exceeding the half-power width of the spatial window for apertures up to 30°. Thus, the variations of telescope signal spectral density with position shown in Figures 10 and 12 to 14 can be interpreted in terms of equation (24) without large error. This is also suggested by results obtained using multiplicative processing [8]. It is intended to use estimates of the coherence between telescope signals to provide a quantitative assessment of the correlation of equivalent line source components, by using the analysis of section 4·5 with larger telescope apertures.

6.1. RESULTS FROM A 12·5° APERTURE ARRAY, WITH TELEVISION DISPLAY

The Acoustic Telescope has been used to determine the sound generation characteristics of a Rolls-Royce/SNECMA Olympus engine with various tailpipe configurations. The measurements have covered the whole range of operating conditions and the microphone array has been positioned at various angles to the engine axis and at various distances from it. In this section, some typical results are presented for the nominal 90° position.

Figure 9 shows the microphone array with an aperture of 12·5°, positioned 45 m from the axis of an Olympus engine with an extended tailpipe. The microphones had equal spacing and were 0·1 m above the concrete surface for work in the frequency range from 400 Hz upwards. Signals were recorded on the 14 channel tape recorder at 60 in/s and replayed at $1\frac{7}{8}$ in/s for laboratory analysis. Recordings were made under calm weather conditions. Apparent source distributions were computed for 14 1/10-decades in the range 400 Hz to 8 kHz, using 39 focal positions from 15 m downstream of the nozzle exit position to 5 m upstream. A data segment length of 512 was used.

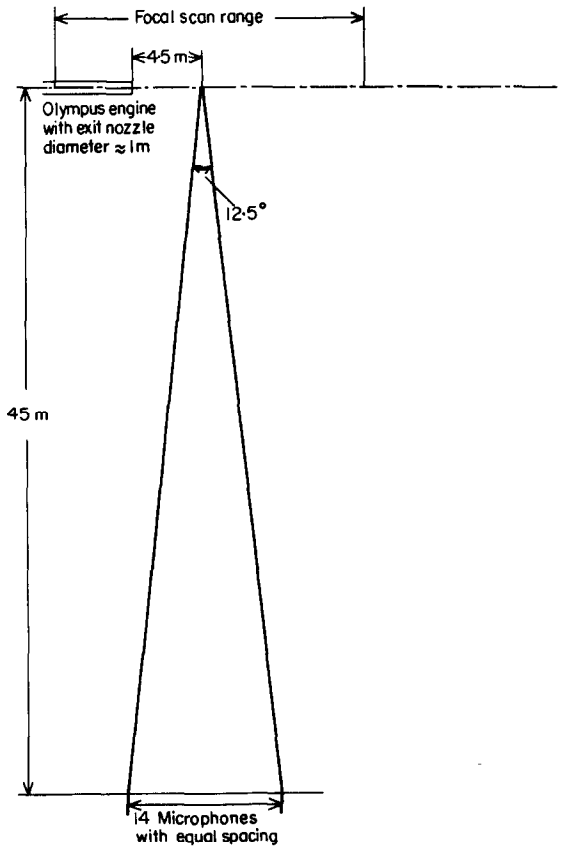

Figure 9. Layout of engine and microphones for tests at Aston Down.

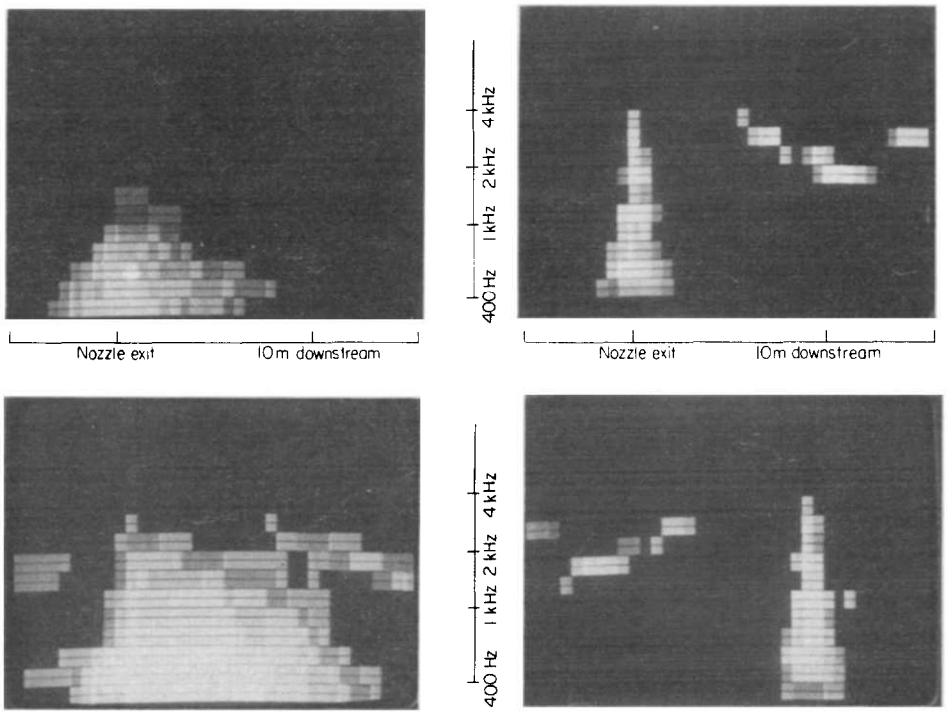

Figure 10. Colour television displays for loudspeaker calibrations and 2 engine conditions. Top left, loudspeaker 1; Bottom left, loudspeaker 2. Top right, low power; Bottom right, high power.

Figure 10 shows the television presentation of the apparent source distributions for the loudspeaker at 0·5 m and 9·0 m downstream of the nozzle exit, obtained from 10 data segments. These are compared with the distributions for the engine at low and high power settings, for 10 and 25 data segments, respectively. The colour steps were chosen so that black and white photography gives increasing brightness with source intensity. In this case, maximum brightness corresponds to a range of 4·5 dB from the highest computed value, with steps of 1·5 dB for each shade of grey.

It can be seen that for the low power condition, the dominant source is close to the nozzle exit, but there are significant sources extending several metres downstream of the nozzle exit (the exit diameter was 0·9 m). At the high power condition, the sources appear farther downstream, with a dominant region from 2 to 8 m downstream of the nozzle exit. These results are in good agreement with those obtained by using two microphones and Binaural Source Location [3, 18].

At the upper end of the frequency range investigated, aliases of the apparent source region can be seen. Their positions are in good agreement with those predicted by using the theory of section 4.2 and have spacing of about 60λ. The apparent half-power width of a monopole source is approximately $3{\cdot}7\lambda$.

At lower frequencies, higher resolution may be required. The following sets of results were obtained by using an array aperture of 30°, with equal cosine spacing of microphones (section 4.2).

6.2. EXPERIMENTS WITH AN ARRAY APERTURE OF 30°

Figure 11 shows a microphone configuration used for tests on an Olympus engine without the flight nacelle which includes the secondary nozzle system. The microphones were 30 m away from the engine axis, with the centre of the array opposite a point 5 m downstream of the

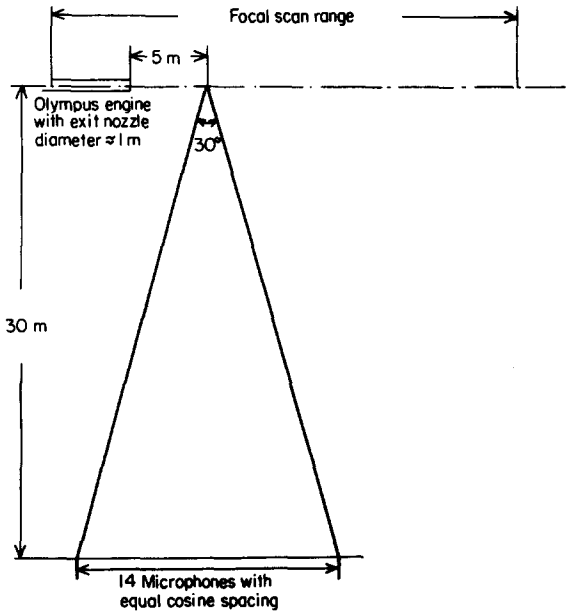

Figure 11. Layout of engine and microphones for tests at Istres.

nozzle exit. They were positioned 0·15 m above the concrete surface of the SNECMA noise test site at Istres, France, so that the first ground reflection interference frequency ($\delta_f(y) = \lambda/4$ in section 4.3) was several times the highest frequency of interest in these tests. Microphone signals were recorded at 15 in/s for replay at $1\frac{7}{8}$ in/s as before.

A scan range from 25 m downstream to 5 m upstream of the nozzle exit was used, with 39 equally spaced foci. Strictly this range is too large in relation to the source to microphone distance to allow use of the second order analysis of section 4.2. However, the most significant sources appeared within ±5 m of the central focus, where the approximation is adequate. 1/10th decade smoothing was used, with 512-point data segments.

Figures 12 to 15 show apparent source distributions obtained with a loudspeaker close to the nozzle exit and analysis from 5 data segments and with the engine running at low power (25 segments), maximum power (100 segments) and maximum power with reheat (100 segments) in the frequency range from 100 Hz to 500 Hz. The number of degrees of freedom, n_f, is given at each frequency. The influence of statistical errors is negligible in each case [14], but results for the 1/10th decade at 400 Hz are significantly affected by mains interference from the tape recorder at replay. This was established by using narrow band presentation of the source distributions around 400 Hz. Unfortunately, amplifiers were not available to allow other tape replay speeds, but the problem is absent when on-line analysis is used.

With the configuration shown in Figure 11, the spacing of aliases is about 25λ and the apparent half-power width of a monopole source is $1{\cdot}6\lambda$. The influence of aliasing can be observed in the apparent distributions for 315 Hz to 500 Hz. Its influence is obvious in these cases, but use of the microphone array at different apertures allows a more thorough study where required. In each test, the source distributions are scaled according to the largest computed value of source intensity with respect to position and frequency. At the maximum power condition shown in Figure 14, this value was outside the frequency range shown.

Figures 13 to 15 show substantial changes with respect to engine power setting commensurate with those shown in Figure 10. However, a comparison of results for full power, with and without reheat shows changes in the relative levels of sources close to the nozzle exit and those further downstream. When reheat is lit, the secondary nozzle-based source becomes

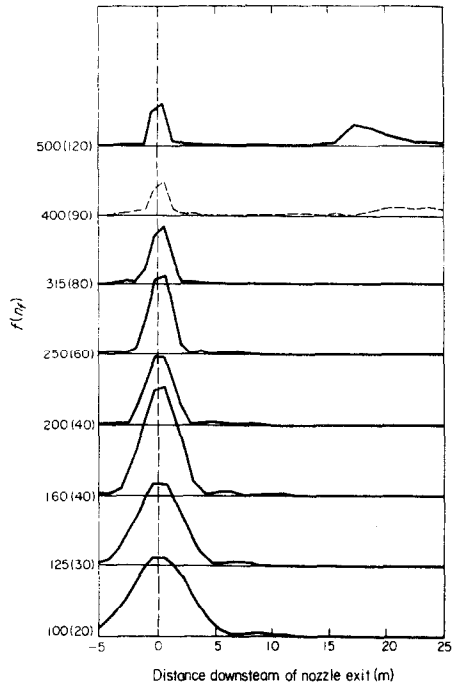

Figure 12. Apparent source distributions of a loudspeaker close to the nozzle exit for 1/10 decade frequency ranges from 100 Hz to 500 Hz, for the arrangement of Figure 11 and 5 data segments. The result for 400 Hz is known to be corrupted by mains hum and is shown dotted. The 1/10 decade centre frequency and n_f are shown.

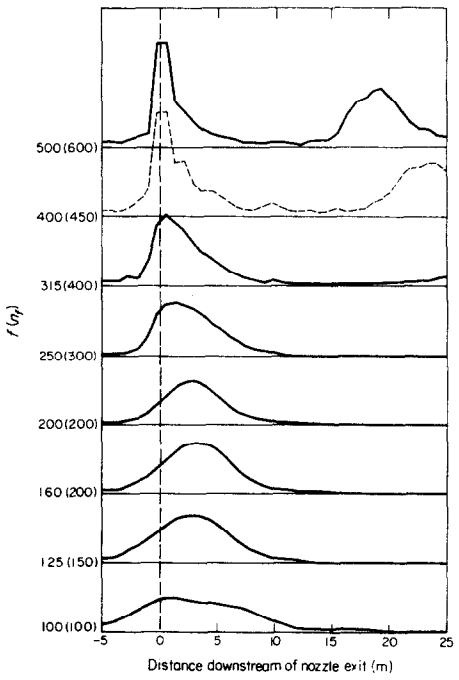

Figure 13. Apparent source distributions of an Olympus engine at low power, for 25 data segments and the arrangement shown in Figure 11. Notation as in Figure 12.

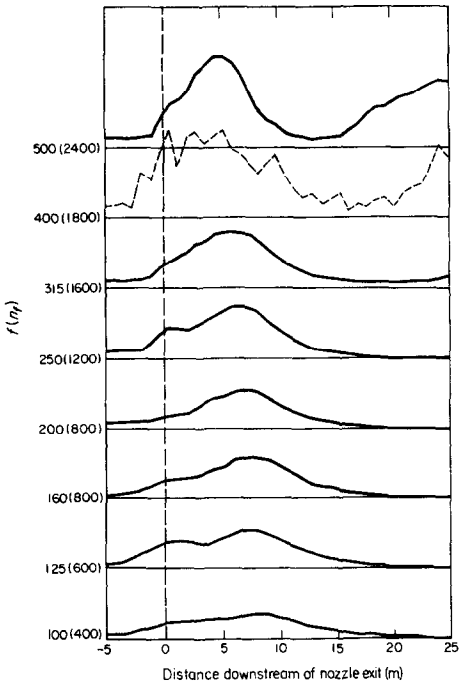

Figure 14. Apparent source distributions of an Olympus engine at full power, for 100 data segments and the arrangement shown in Figure 11. Notation as in Figure 12.

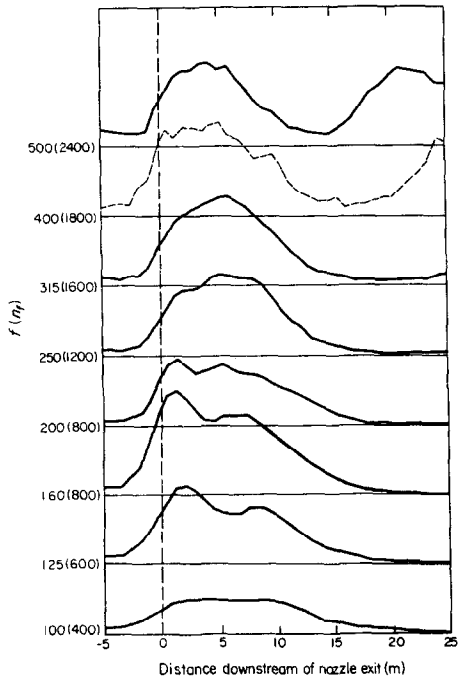

Figure 15. Apparent source distributions of an Olympus engine at full power with reheat, for 100 data segments and the arrangement shown in Figure 11. Notation as in Figure 12.

more obvious at low frequencies, but the overall effect is about that expected from the increase in jet velocity, owing to the limited frequency range over which the secondary source is prominent. Even at frequencies between 100 Hz and 200 Hz, it would not be expected to increase noise levels by more than a few dB, but its practical importance is further diminished on the PNdB scale, where low frequencies are given reduced weighting.

These results illustrate how the Acoustic Telescope can provide information about the characteristics of a sound producing region. It has been particularly valuable in exploring the effects of changes in the engine configuration and in establishing the apparent origin of sound at various far-field positions in the rearward and forward arcs.

7. CONCLUSIONS

A complete system, based on an array of 14 microphones and a mini-computer, has been developed for sound source location on jet engines. This "Acoustic Telescope" can be used on-line with a variety of computational and display techniques for rapid presentation of results and was designed for interactive use by engineers without specialized knowledge of computers. It can be transported in an estate car for field studies, or a tape recorder can be used as a link between the test site and the computer system.

The basic properties of the system are introduced via an empirical analysis. This is complemented by a frequency domain analysis for the case of a line source of arbitrarily correlated monopoles. It is shown how additive processing of signals from a fixed array leads to presentation of a measure of sound source intensity as a function of position and frequency. The application of the system for the estimation of the statistical properties of a source region is considered in detail, including its uses to determine the correlation of different parts of the region, in the presence of ground reflections and atmospheric defects and in a wind tunnel.

The system was applied to tests on an Olympus engine and some typical results are presented in television display and plotter formats. It is shown how the apparent sources are close to the nozzle exit at low power settings, but are further downstream at high power. In the latter case, the most significant region of sound generation appears to be between 3 and 9 nozzle diameters downstream. The array is calibrated by using a loudspeaker in two or more known positions in order to ensure correct functioning under prevailing environmental conditions.

Although its main application so far has been the determination of the statistical properties of a source region, the Acoustic Telescope can also be used to resolve the individual events which lead to the overall properties. For instance, it can be used to study sources in motion, or to study such phenomena as "crackle" which are not amenable to conventional noise analysis techniques.

The computer programs for the Acoustic Telescope were developed to give maximum flexibility with FORTRAN programming using a library of subprograms written in assembly language for high performance. The ease with which both hardware and software configurations can be altered gives the Acoustic Telescope an important advantage over source location techniques which have to be restricted to one type of analysis. Although the number of microphones was restricted to 14 for the experimental results presented in this paper, the system performance is adequate for handling up to 32 microphone signals.

ACKNOWLEDGMENTS

The work was carried out under the direction of Professor J. E. Ffowcs Williams and supported by the Bristol Engines Division of Rolls-Royce (1971) Limited. The authors are grateful for the enthusiastic support of Professor Ffowcs Williams and for the contributions of J. L. Moughton, who was responsible for a substantial part of the computer system

development, O. E. Flynn, J. R. Jacques and O. J. Whitfield. The assistance of B. L. Wootton and his staff in the Control Engineering Laboratory at Cambridge is gratefully acknowledged. The authors appreciated the support of R. Hawkins and R. Hoch and their colleagues in Rolls-Royce and SNECMA noise departments.

REFERENCES

1. J. E. Ffowcs Williams 1974 *AGARD Technical Evaluation Report AR*-66. Noise mechanisms.
2. F. R. Grosche 1973 *AGARD Conference Proceedings CP*-131. Distributions of sound source intensities in subsonic and supersonic jets.
3. R. Kinns 1976 *Journal of Sound and Vibration* **44**, 275–289. Binaural source location.
4. M. J. Fisher and M. Harper Bourne 1974 *Aeronautical Research Council Report ARC* 35/383/*N*910. Source location in jet flows.
5. A. Clemons, M. Hehmann and K. Radecki 1973 *NASA Contractor Report CR*-134499/*R*73 *AEG* 443, Vols I and II. Quiet engine program turbine noise suppression.
6. J. Billingsley 1974 *Aeronautical Research Council Report ARC* 35/364. An acoustic telescope.
7. R. Kinns and J. Billingsley 1975 *Aeronautical Research Council Report ARC* 36/109/*N*978. Application of the acoustic telescope to noise measurements on a Viper engine, with considerations on the theory and development of the telescope.
8. O. E. Flynn and R. Kinns 1976 *Journal of Sound and Vibration* **46**, 137–150. Multiplicative signal processing for sound source location on jet engines.
9. R. Kinns 1973 *International Journal for Numerical Methods in Engineering* **6**, 395–411. Spectral analysis on a small computer.
10. P. D. Welch 1967 *Institute of Electrical and Electronic Engineers Transactions on Audio and Electroacoustics AU*-**15**, 70–73. The use of the fast Fourier transform for the estimation of power spectra; a method based on time averaging over short, modified periodograms.
11. R. Kinns 1973 *Journal of Sound and Vibration* **26**, 121–128. Aliasing in the time domain for the estimation of power spectra.
12. J. S. Bendat and A. G. Piersol 1971 *Random Data: Analysis and Measurement Procedures.* New York: J. Wiley & Sons, Inc.
13. G. C. Carter, C. H. Knapp and A. M. Nuttal 1973 *Institute of Electrical and Electronic Engineers Transactions on Audio and Electroacoustics AU*-**21**, 388. Statistics of the estimate of the magnitude-coherence function.
14. R. Kinns 1975 *Cambridge Noise Research Unit Memorandum RK*/63. Tests on the statistical stability of source distributions.
15. M. E. Delany 1969 *NPL Aero Special Report* 033. Range prediction for siren sources.
16. M. S. Howe 1973 *Cambridge Noise Research Unit Memorandum MSH*/6. Proposal for discussion on scanning techniques for increasing the resolution of the CNRU acoustic telescope.
17. J. M. Fitremann and J. E. Ffowcs Williams 1973 *Cambridge University Engineering Department Report.* Spectral broadening and variability of discrete turbine tones propagating through unsteady flow.
18. R. Kinns 1976 To be published. Experiments using binaural source location.

APPENDIX: NOTATION

c	speed of sound in atmosphere
d	separation of microphone array and assumed line of source
f	frequency
i	$\sqrt{-1}$
j	microphone index
k	sample number
$l_j(y)$	distance from the source at y to the jth microphone
$l_j(y_0)$	distance from the telescope focus at y_0 to the jth microphone
n_f	number of degrees of freedom of power and cross-spectral density estimates
$p_j(t)$	signal received from the jth microphone at time t
$q(y,t)$	line source density at position y and time t
$s(k,j)$	kth sample of the signal from the jth microphone
t	time

w_{0j} weighting factor for the signal from the jth microphone after compensation for propagation distance
y distance along line of sources from specified origin
y_0 distance of focal position from origin on line of sources
C_0, C_1, C_2 spatial windows
M Mach number
N number of microphones
$P_{ss}(y_0', f)$ power spectral density of telescope signal at frequency f for focal position y_0
$P_{ss'}(y_0, y_0', f)$ cross-spectral density of telescope signals for focal positions y_0 and y_0'
$Q(y, f)$ Fourier transform of $q(y,t)$: $\int_{-\infty}^{\infty} q(y,t)e^{-2\pi i f t}\,dt$
$Q_{yy'}(f)$ cross-spectral density of source densities at positions y and y', at frequency f
$Q'_{yy'}(f)$ modified cross-spectral density (equation (16))
$\bar{R}'(y, f)$ effective source intensity: $\int_{-\infty}^{\infty} \mathrm{Re}\,[Q'_{yy'}(f)]\,dy'$
$S(y_0, t)$ telescope signal for focal position y_0 at time t
$S_n(k)$ kth sample from the telescope signal for the nth focal position
Δ spacing in $\cos(\theta_j)$ for case of equal cosine spacing between microphones
θ_j angular position of jth microphone
λ wavelength of sound in atmosphere